Received: 24 April 2018 | Revised: 13 July 2018 | Accepted: 13 July 2018

DOI: 10.1111/fog.12406

ORIGINAL ARTICLE

WILEY FISHERIES OCEANOGRAPHY

Response of Scotian Shelf silver hake (*Merluccius bilinearis*) to environmental variability

Daniel Reed[1] | Stéphane Plourde[2] | Adam Cook[1] | Pierre Pepin[3] | Benoit Casault[1] | Caroline Lehoux[2] | Catherine Johnson[1]

[1]Fisheries and Oceans Canada, Bedford Institute of Oceanography, Dartmouth, Nova Scotia, Canada

[2]Pêches et Océans Canada, Institut Maurice-Lamontagne, Mont-Joli, Quebec, Canada

[3]Fisheries and Oceans Canada, Northwest Atlantic Fisheries Centre, St. John's, Newfoundland and Labrador, Canada

Correspondence
Catherine Johnson, Fisheries and Oceans Canada, Bedford Institute of Oceanography, 1 Challenger Drive, PO Box 1006, Dartmouth NS B2Y 4A2, Canada.
Email: Catherine.Johnson@dfo-mpo.gc.ca

Funding information
Fisheries and Oceans Canada

Abstract

Commercially-exploited fish populations are not only shaped by fishing pressure, but also by the dynamics of their environment. By quantifying the influence of environmental variability, fisheries management advice can be improved and uncertainties reduced. To this end, we developed statistical models of the response of Scotian Shelf silver hake stock metrics to variability in zooplankton community composition and phenology over the past 18 years and in the physical environment since 1985. Dominant modes of variability in these pelagic habitat indicators were characterized using principal component analysis, and the relationships of silver hake condition, abundance, and recruitment to pelagic habitat variability were assessed using generalized additive models. Condition was largely modulated by the onset and duration of the spring bloom, which controls food availability. In contrast, adult abundance was governed by composition of the zooplankton community and bottom-water temperature, which dictates the distribution of silver hake. Finally, recruitment was affected by both thermal conditions and food availability. Our results presented here form the basis for qualitative assessment of ecosystem attributes and the influence on silver hake stock productivity.

KEYWORDS
adult abundance, condition, environmental variability, generalized additive models, recruitment, Scotian Shelf, silver hake

1 | INTRODUCTION

Key attributes of fish stocks (e.g., condition, abundance, recruitment) are shaped by fishing pressure, variability in the physical environment, and the dynamics of the prey upon which they depend. However, many stock assessments do not account for environmentally-driven processes (Skern-Mauritzen et al., 2016), as relationships between fish metrics and environmental conditions are often poorly understood (Myers, 1998). Quantitatively linking stock metrics to environmental variability would help inform fisheries management advice (Brown, Fulton, Possingham, & Richardson, 2012), in addition to providing insight into potential shifts in population structure and condition as a result of environmental change. Nevertheless, despite their importance, it has proven difficult to establish such quantitative links in practice (Rose, 2000).

Validating hypothesized relationships between individual environmental indices and fish stock metrics has proven largely unsuccessful due, in part, to the interactions among multiple processes that influence these communities simultaneously, nonlinear relationships, and weak and transient responses (Myers, 1998). An alternative approach

This is an open access article under the terms of the Creative Commons Attribution License, which permits use, distribution and reproduction in any medium, provided the original work is properly cited.
© 2018 Her Majesty the Queen in the Right of Canada. Fisheries Oceanography © 2018 John Wiley & Sons Ltd. Reproduced with the permission of Fisheries and Oceans Canada

is to characterize the dominant modes of environmental variability using multivariate analyses of an ensemble of indices and then to relate these modes to fish stock metrics while making minimal a priori assumptions about the explicit linking processes (Brosset et al., 2018; Hare & Mantua, 2009; Plourde et al., 2015). While this approach was originally applied in the Northwest Atlantic to mackerel recruitment in the Gulf of St. Lawrence, the overarching philosophy is generic and readily adapted for other pelagic fish stocks. Here, we apply this approach to the silver hake (*Merluccius bilinearis*) stock on the Scotian Shelf (Figure 1). This stock is an excellent candidate for examining the influence of environmental factors on stock attributes as fishing pressure is low, with landings only half of the total allowable catch in recent years (DFO, 2017). Although Scotian Shelf silver hake are presently not fished extensively, the population has supported a substantial fishery in the past. Recorded commercial exploitation of silver hake on the Scotian Shelf began in 1963 with fishing intensifying in the early 1970s (Rikhter, Sigaev, & Vinogradov, 2001). Landings subsequently declined substantially after the exclusive economic zone was established in the region in 1977, and regulatory policies were introduced that reduced the area of the fishery by approximately 90%, restricted bycatch, and shortened the silver hake fishing season (Rikhter et al., 2001). This, together with a low market demand, has led to an underexploited fishery and a relatively low fishing pressure (DFO 2017; Figure S1). The decline in fishing pressure has reduced the importance of a potentially confounding factor and, as a result, provides the opportunity to link variation in the population to variation in its pelagic environment, which is the subject of the present communication.

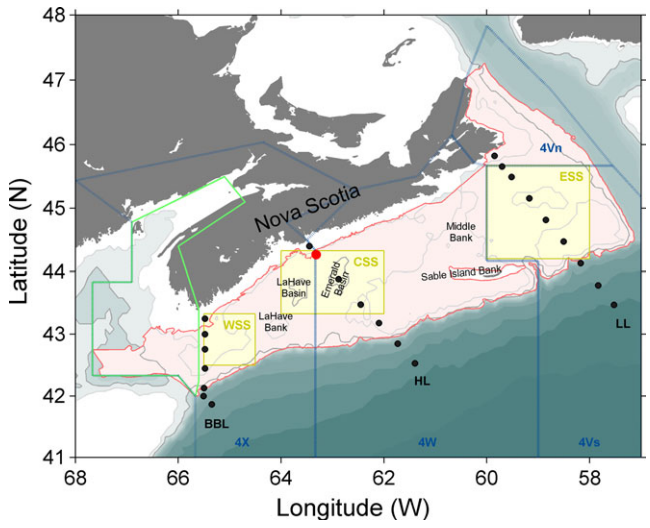

FIGURE 1 Scotian Shelf subregions relevant to this study. Plotted on the map are the following: NAFO regions (4X/W/Vs/Vn; blue lines), eastern Gulf of Maine and Bay of Fundy (eGoM+BoF; green box); western, central, and eastern Scotian Shelf boxes for satellite data (WSS, CSS, ESS, respectively; yellow boxes); strata 440–483 for the summer research vessel survey (red polygon); Browns Bank Line (BBL), Halifax Line (HL), Louisbourg Line (LL) sections (black circles), and station Halifax 2 (HL2; red circle)

There are several well-established features of silver hake ecology that we would expect to see manifested in this analysis. Silver hake typically inhabit warm bottom waters around 5–10°C (Sigaev, 1994). In the summer, waters off the coast of Nova Scotia stratify into a three-layer structure that includes warm surface waters, a cold intermediate layer (CIL) formed through wind-driven mixing in the winter and influenced by advection from the Gulf of St. Lawrence and other upstream sources, and warm, saline deep water advected onto the shelf from Gulf Stream-influenced slope waters (Gatien, 1976; McLellan, 1957; McLellan, Lauzier, & Bailey, 1953; Petrie, Smith, Petrie, & Smith, 1977; Smith, Petrie, & Mann, 1978). Silver hake prefer warm slope waters and, consequently, their distribution is expected to be influenced by climatic processes that shift the position of large-scale hydrological boundaries such as the Gulf Stream north wall (e.g., Nye, Joyce, Kwon, & Link, 2011). The composition of the zooplankton community also influences silver hake condition and abundance through availability of preferred prey. Euphausiids (krill) constitute a large part of adult silver hake's diet (Clay, Currie, & Swan, 1984), and we would therefore anticipate a positive relationship between krill abundance and silver hake condition and abundance. As recruitment could be, in part, a function of abundance and condition of adults, in addition to environmental conditions, recruitment may in turn be correlated with krill abundance. Conversely, negative correlations have been observed between silver hake catches and the abundance of copepods at catch location ("Calanoids" in Sigaev, 1994). While the mechanism linking silver hake and copepod abundances is yet to be established, it is possible that these species act as a proxy for water masses as *Calanus* spp. prefer colder waters. We anticipate that these factors—krill and copepod abundances, bottom-water temperature, together with factors yet to be identified—shape characteristics of the silver hake population.

Environmental attributes vary on multiple time scales, compounding or countering one another, and thus eliciting complex responses within fish populations. Here, we seek to disentangle these signals by analyzing an 18-year time series (1999–2016) describing zooplankton community composition, phenology, and silver hake stock metrics (i.e., condition, adult abundance, recruitment), as well as a data set of physical indices stretching back to 1985. Using statistical models, we identify and quantify the most pertinent drivers of variability for the silver hake population and establish common factors linking interannual variability in condition, abundance, and recruitment. We conclude by considering these results in the context of fisheries management.

2 | METHODS

The overarching approach adopted here follows Plourde et al. (2015). In brief, data sets are constructed to characterize the dominant modes of variability in zooplankton community composition, phenology, and environmental conditions in the region, using principal component analysis (PCA). The first three principal components (PCs) of each PCA, which represent most of the variability, are then

TABLE 1 Variables included in the principal component analyses

Variable	Group	Period
July bottom temperature (4X, 4W, 4V)	Physical	1985–2016
Sea-surface temperature, January–December, except 4V April–December (4XSS, 4W, 4V, Gulf of Maine + Bay of Fundy)	Physical	1985–2016
North Atlantic Oscillation (NAO) index	Physical	1985–2016
Atlantic Multidecadal Oscillation (AMO) index	Physical	1985–2016
Annual mean St. Lawrence river flux	Physical	1985–2016
Cold intermediate layer (CIL) volume (August–September; Scotian Shelf)	Physical	1985–2016
Mean ice volume (January–February–March; Gulf of St. Lawrence + Scotian Shelf)	Physical	1985–2016
Stratification (Scotian Shelf)	Physical	1985–2016
Calanus finmarchicus	Zooplankton	1999–2016
Calanus hyperboreus	Zooplankton	1999–2016
Calanus glacialis	Zooplankton	1999–2016
Pseudocalanus spp.	Zooplankton	1999–2016
Metridia longa	Zooplankton	1999–2016
Metridia lucens	Zooplankton	1999–2016
Metridia spp.	Zooplankton	1999–2016
Temora spp.	Zooplankton	1999–2016
Microcalanus spp.	Zooplankton	1999–2016
Oithona spp.	Zooplankton	1999–2016
Oithona similis	Zooplankton	1999–2016
Oithona atlantica	Zooplankton	1999–2016
Paracalanus spp.	Zooplankton	1999–2016
Centropages typicus	Zooplankton	1999–2016
Centropages spp.	Zooplankton	1999–2016
Scolecithricella minor	Zooplankton	1999–2016
Larvacea	Zooplankton	1999–2016
Gastropoda	Zooplankton	1999–2016
Bivalvia	Zooplankton	1999–2016
Euphausiacea	Zooplankton	1999–2016
Sea-surface temperature warming (March–May)	Phenology	1999–2016
Final day of sea ice (Gulf of St. Lawrence + Scotian Shelf)	Phenology	1999–2016
Mean ice area (Gulf of St. Lawrence + Scotian Shelf; January–March)	Phenology	1999–2016
Annual peak in *Calanus finmarchicus* biomass (Station HL2)	Phenology	1999–2016
Annual peak in proportion of *Calanus finmarchicus* life stages I+II+III relative to total population	Phenology	1999–2016
Annual peak in total zooplankton biomass (Station HL2)	Phenology	1999–2016
Start of phytoplankton bloom (eastern, central, and western Scotian Shelf)	Phenology	1999–2016
Duration of phytoplankton bloom (eastern, central, and western Scotian Shelf)	Phenology	1999–2016

used together as predictors in a suite of generalized additive models (GAMs) of fish condition (i.e., weight at length), adult abundance, and recruitment. These GAMs consider all possible combinations of PCs with a maximum of three terms per model to prevent overfitting. The top models in the suite of GAMs are then identified using the Akaike information criterion (AIC). This approach is described in detail below.

2.1 | Data assembly

Silver hake stock metrics were obtained using data from Fisheries and Oceans Canada's (DFO) summer research vessel surveys (RV survey hereafter). This stratified random bottom trawl survey has been conducted annually in July and August since 1970. The survey trends are considered representative of the silver hake stock status (Stone, Themelis, Cook, & Clark, 2013). During the course of the RV survey time series, there have been several changes in trawl methodology, but none of these occurred during the time period of analyses conducted here and were therefore ignored. Although the survey covers the Scotian Shelf and the Bay of Fundy (Figure 1), the commercial silver hake stock is largely contained within the Scotian Shelf and, consequently, indicators were estimated for strata 440–483 (Figure 1, region bounded by the red line). The stock metrics for silver hake estimated from the survey were fish condition (i.e., weight at length), stratified adult abundance, and stratified recruit abundance. The size of silver hake recruiting to the Scotian Shelf fishery was 19 cm total length, with individuals from 10 to 18 cm providing an estimate of those which would be entering the adult and commercial population within the year (Stone et al., 2013). Fish condition was estimated for adult silver hake using the stratified mean weight at 25 cm. One sample t-tests revealed no significant difference between males and females over the time series (p value: 0.9), suggesting that our metric of condition is not affected by spawning seasonality or survey timing. Adult abundance and condition metrics were included in the analysis rather than biomass to address population size and condition as separate qualities of the stock, rather than conflating these attributes into a single metric.

Environmental variables representing pelagic habitat status in the region were assembled (Table 1) using data products from the Atlantic Zone Monitoring Program (AZMP; Therriault et al., 1998; Mitchell et al., 2002). While the approach adopted here is based on Plourde et al. (2015), we employ a more comprehensive data set in an effort to better characterize the pelagic habitat. Pelagic habitat status metrics included groups of variables representing the physical

environment, zooplankton community composition, and phenology—that is, the timing of periodic biological events (Table 1; referred to as physical, zooplankton, and phenology, respectively, henceforth). Silver hake in the Northwest Atlantic are known to be influenced by shifts in the position of the Gulf Stream (Nye et al., 2011), and catch biomass is correlated with near-bottom temperature and the composition of the zooplankton community (Sigaev, 1994). The pelagic habitat database was intended to quantify interannual variability in these aspects of the habitat and in the timing of key seasonal events. The 39 variables used in the analyses are described in detail below.

Variability in the physical environment was assessed using annual metrics for bottom temperature, sea-surface temperature (SST), large-scale climate indices, freshwater inputs upstream, winter conditions, and stratification. Metrics representing each of these characteristics of the physical environmental, described below, were estimated by Hebert, Pettipas, Brickman, and Dever (2016). The full set of physical environmental metrics was available from 1985 to 2016, although data were unavailable for 1988 and 1989 (Hebert et al., 2016). July bottom-water temperatures were averaged spatially based on Northwest Atlantic Fisheries Organization (NAFO) regions 4X, 4W, and 4V, bounded by the 200 m isobath along the shelf break, while SSTs were averaged over spatial regions defined by the shelf portions (i.e., <200 m) of regions 4XSS (January–December), 4W (January–December), and 4V (April–December), as well as for the combined Gulf of Maine (GoM) and Bay of Fundy (BoF) (January–December) (Figure 1). Large-scale climate processes were represented in the data set by indices for the North Atlantic Oscillation (NAO) and Atlantic Multidecadal Oscillation (AMO). The index for the NAO is the difference in the atmospheric pressure at sea level between two contrasting stable pressure systems in the North Atlantic, the Azores high and Icelandic low (Hurrell, 1995), while the AMO index is a detrended weighted-average of SST across the entire North Atlantic (Sutton & Hodson, 2013) and has a period of about 65–70 years (Schlesinger & Ramankutty, 1994). The magnitude of the St. Lawrence River flux was also included to represent precipitation and freshwater inflow upstream of the Scotian Shelf. In summer, the Scotian Shelf water column is structured into three distinct layers, with the coldest water at intermediate depths defining the CIL. The CIL is formed through winter cooling of the upper water column and wind-driven mixing followed by surface warming in spring and summer. CIL volume and combined ice volume for the Gulf of St. Lawrence and Scotian Shelf were used to characterize winter conditions that are the start point for the spring production cycle in the region. Finally, an annual-scale stratification index for the Scotian Shelf was also included, defined as the difference in density (i.e., $\Delta\sigma_T$) between near-surface waters and those at 50 m depth (Hebert et al., 2016).

Zooplankton community variability was assessed using normalized annual abundance anomalies (Johnson, Devred, Casault, Head, & Spry, 2018; reference period 1999–2010) for the dominant and subdominant copepods, and dominant noncopepod groups, including euphausiids, collected at three Scotian Shelf sections (Browns Bank Line, Halifax Line, Louisbourg Line) and at the time series station at Halifax Line Station 2 (HL2; Figure 1) on the inshore central Scotian Shelf for the interval 1999–2016 (Table 1). Zooplankton were collected with a 0.75 m ring net equipped with 202 μm mesh, towed vertically from near-bottom to the surface, and analyzed according to methods outlined in Mitchell et al. (2002). Adults and copepodids of the copepod genus *Calanus* were identified to species and developmental stage in most cases, and the sum of all adult and copepodid stages was included in the analysis. For other copepod genera, adults were typically identified to species, while earlier copepodid stages were identified only to genus. For copepod genera represented by only one species throughout the region (*Paracalanus* sp., *Temora* sp.) or genera not identified to species (*Pseudocalanus* sp., *Microcalanus* sp.), genus and species abundances were summed and noted as genus. For genera represented by multiple species, adult abundances and copepodite abundances were presented separately. Total zooplankton biomass was estimated as water column-integrated wet mass (g/m^2).

Different zooplankton taxa fill different ecological niches, and their presence may thus be indicative of specific environmental conditions. *Calanus* and *Pseudocalanus* species in this region are north temperate (*Calanus finmarchicus*) or arctic (*Calanus hyperboreus* and *Calanus glacialis*) copepods with production typically associated with the spring phytoplankton bloom. In contrast, *Paracalanus* sp. and *Centropages* sp. are shallow-water copepods that favor warmer conditions in the summer and fall, while *Microcalanus* sp. and *Metridia* sp. are detritivorous copepods typically associated with deep shelf waters. *Oithona* species are broadly distributed generalist feeders, and *Scolecithricella minor*, which are also detritivores, are mainly associated with slope waters in the study region. Euphausiid juveniles and adults are not well sampled under the AZMP sampling design (vertical ring net tows, sections) due to their strong swimming ability and patchy distributions. However, the abundances of euphausiids captured by the ring nets, which are mainly early stages, were considered here to be an indicator of their population levels, in the absence of other sources of data on euphausiid interannual variability.

Variability in the timing of biological events on the Scotian Shelf between 1999 and 2016 was assessed using several phenology metrics that represent rate of spring warming, final day and mean area of sea ice, timing of spring peaks in total *C. finmarchicus* abundance, abundance of early life stages of *C. finmarchicus*, and zooplankton biomass, and the onset and duration of the spring phytoplankton bloom. Like the zooplankton metrics, normalized annual anomalies were calculated for each phenology metric, with a reference period of 1999–2010. The rate of surface warming was calculated as the slope of a linear regression fit to bimonthly SST values over decimal months for March, April, and May, using bimonthly means for SST from NOAA's Advanced Very High Resolution Radiometer (AVHRR). SST warming rate metrics were calculated for standard boxes representing conditions on the eastern, central and western Scotian Shelf (ESS, CSS, and WSS, respectively; Figure 1), corresponding to the Louisbourg, Halifax, and Browns Bank sections, respectively. The last

day of sea ice was estimated over a 0.1° × 0.1° grid covering the area between 65°W to 40°W and 43°N to 55°N and mean ice area for the Scotian Shelf and Gulf of St. Lawrence was calculated over January, February, and March. Seasonal dynamics of the zooplankton community on the Scotian Shelf were quantified using data from HL2, which is nominally sampled twice monthly. The timing of the maximum abundance of *C. finmarchicus*, the dominant copepod species by biomass, and the timing of maximum zooplankton biomass were both determined by fitting a LOESS curve with a span parameter of 0.7 to log-transformed data for each year using the *loess* function of the *stats* package for R (R Development Core Team 2016). While the timing of the zooplankton biomass peak is often similar to the peak in *C. finmarchicus*, including both metrics allows deviations between the two metrics related to shifts in the zooplankton community to be represented in the analysis. The LOESS approach did not perform well when quantifying the timing of *C. finmarchicus* production (i.e., peak abundance of life stages CI–III). We therefore performed a PCA on the relative abundance of the six copepodite stages of *C. finmarchicus* to determine the timing of the peak in the early copepodite stages (I through III), as a proxy for the peak of production. Loadings on the first principal component (PC) of the analysis showed that this provided a good description for these early life stages (47% of variance explained) and, consequently, the peak in PC1 was used as the metric for the timing of the peak *C. finmarchicus* production. Other key aspects of plankton phenology included in the data set were the initiation (day of year) and duration (days) of the spring phytoplankton bloom in the ESS, CSS, and WSS regions (Figure 1), which were derived from SeaWiFS (Sea-viewing Wide Field-of-view Sensor) data for 1999–2008 and MODIS (Moderate-resolution Imaging Spectroradiometer) data for 2009–2016 (Johnson et al., 2018). These parameters were determined using the shifted Gaussian function of time model (Johnson et al., 2018; Zhai, Platt, Tang, Sathyendranath, & Herna, 2017).

2.2 | Analysis

A PCA was performed on each of the groups of environmental variables to derive a small number of orthogonal variables that explained the bulk of the variance, while revealing dominant variability modes. PCA was performed using the *prcomp* function of the *stats* package for R, and variables were centered and scaled prior to undertaking the analysis (R Development Core Team 2016). Zooplankton abundances were log-transformed prior to centering and scaling. The first three PCs for each group of variables were then used as predictors in GAMs describing fish condition, abundance, and recruitment. We adopted the following model formulation:

$$g(E(y)) = \eta = \beta_0 + \sum_{i=1}^{n} f_i(x_i) + \varepsilon$$

where y is the dependent variable (i.e., fish stock metric) and x_i represents the ith independent variable (e.g., PCs), f_i is a smoothing function for covariate x_i, β_0 is the intercept of the model, n is the number of covariates, and η is the predictor, which is associated with the expected value of y through a link function, g. Here, we use an identity link function and Gaussian distribution of the response variable ($\varepsilon \sim N(0, \sigma^2)$). Like Plourde et al. (2015), we also included total silver hake biomass as a predictor in models for condition to allow for density-dependent effects. Similarly, total adult biomass was included as a predictor for recruitment abundance, as a relationship between these variables has previously been established (Rikhter et al., 2001). To prevent overfitting, a maximum of three terms were used per GAM (i.e., $n \leq 3$) and smoothers had a maximum of three knots. All possible combinations of predictors were used, and GAMs were fit using the *gam* function from the R package *mgcv* (Wood, 2006). Models with concurvity coefficients greater than 0.5 were omitted (Wood, 2006). We considered concurvity rather than a metric of linear correlation (e.g., Pearson's correlation coefficient between PCs, Figure S2) as smoothed terms in GAMs are not necessarily linear, yet may still be correlated. Concurvity can only be assessed after model fitting and, consequently, all possible models must be fit and then filtered according to their concurvity coefficients. For each model, percentage of deviance explained, generalized cross-validation (GCV) statistic, and AIC were calculated. To determine which models performed best, GAMs were ranked according to AIC, which provides a measure of goodness of fit while accounting for model complexity. We considered the top five models to identify common terms that explained the majority of variability. The top-ranking model is referred to as the "optimal" model hereafter. In addition, the magnitude of each term in the optimal model was calculated and plotted over the time series to provide insight into its role in the model (e.g., whether it accounts for interannual variability of a small magnitude or large, episodic shifts).

To assess the validity of the modeling assumptions, we examined the residuals of the optimal models. Q-Q plots were used to ensure that residuals were normally distributed. Linear models were fit to residuals over time using the *lm* function of the R *stats* package to confirm the absence of statistically significant trends by examining the confidence intervals of the gradient using *confint* from the same package. To quantify autocorrelation, a linear model including an AR1 structure was fit to residuals over time using the *gls* function from the *nlme* package and the confidence interval for φ was examined using the *intervals* function from the same package to ensure it encompassed zero. In addition, autocorrelation was calculated as a function of lag using the *acf* function of the *stats* package and plotted for visual inspection.

We validated the optimal models using a bootstrapping approach for the PCA and a jackknife approach for the GAM fitting. For the bootstrapping, each variable in Table 1 was resampled with replacement to generate a random data set upon which a PCA was performed. Optimal GAMs were then refit to the resulting PCs. This procedure was repeated 1,000 times to estimate the distribution of the percentage of deviance explained by the optimal models. For the jackknife analysis, each data point in the fish metrics time series was omitted and all possible GAMs were refit to the remaining data set. These models were then sorted according to AIC to determine whether the optimal model

remained the top-ranking model. Percentage of deviance explained was also calculated for comparison.

To quantify the predictive ability of optimal models, we also performed a leave-one-out cross-validation (LOOCV) where each data point from the fish metrics time series was omitted systematically, the optimal model was refit to the remaining data set, and then, the model was used to predict the value of the omitted point. Differences between observations and predictions were used to calculate mean absolute errors (MAE) for each optimal model.

3 | RESULTS

3.1 | Principal component analyses

The first three PCs of each PCA explained a total of 81.7%, 47.6%, and 78.1% of the variability in the physical, zooplankton, and phenology data sets, respectively. Whereas zooplankton PC1 and physical PC1 show trends over the length of the time series, other PCs were characterized by more complex multiyear or interannual modes of variability (Figure 2). The time series for the physical data was almost 70% longer than those for zooplankton and phenology, which allowed for longer modes of variability to be extracted.

Principal component analysis of the physical data revealed a strong influence of warming and large-scale climate fluctuations on variability. PC1 explained 49% of the variance and reflected a long-term increase in the temperature of both surface and deep waters across all regions, as well as a negative association with CIL and ice volumes—consistent with the warming trend—and positive associations with AMO and NAO indices and stratification (Figure 3a). Physical PC2 accounted for 21.1% of the variance, less than half of PC1, and exhibited a higher frequency of variability than PC1 (Figure 2b). This principal component represented contrasting temperature patterns in surface and deep waters, with positive associations with warmer deep waters and colder surface waters (Figure 3b). Physical PC2 had a strong negative association with AMO index, as well as negative associations with SST of declining magnitude from east to west across the three Scotian Shelf regions, and negative association with CIL volume and stratification (Figure 3b). Physical PC2 was also positively associated with freshwater flux of the St. Lawrence river. Finally, physical PC3, which explained 11.6% of the variance, exhibited strong, distinct, and positive associations with the NAO index and ice volume in the Gulf of St Lawrence and on the Scotian Shelf, as well as a negative relationship with St. Lawrence river flux (Figure 3c).

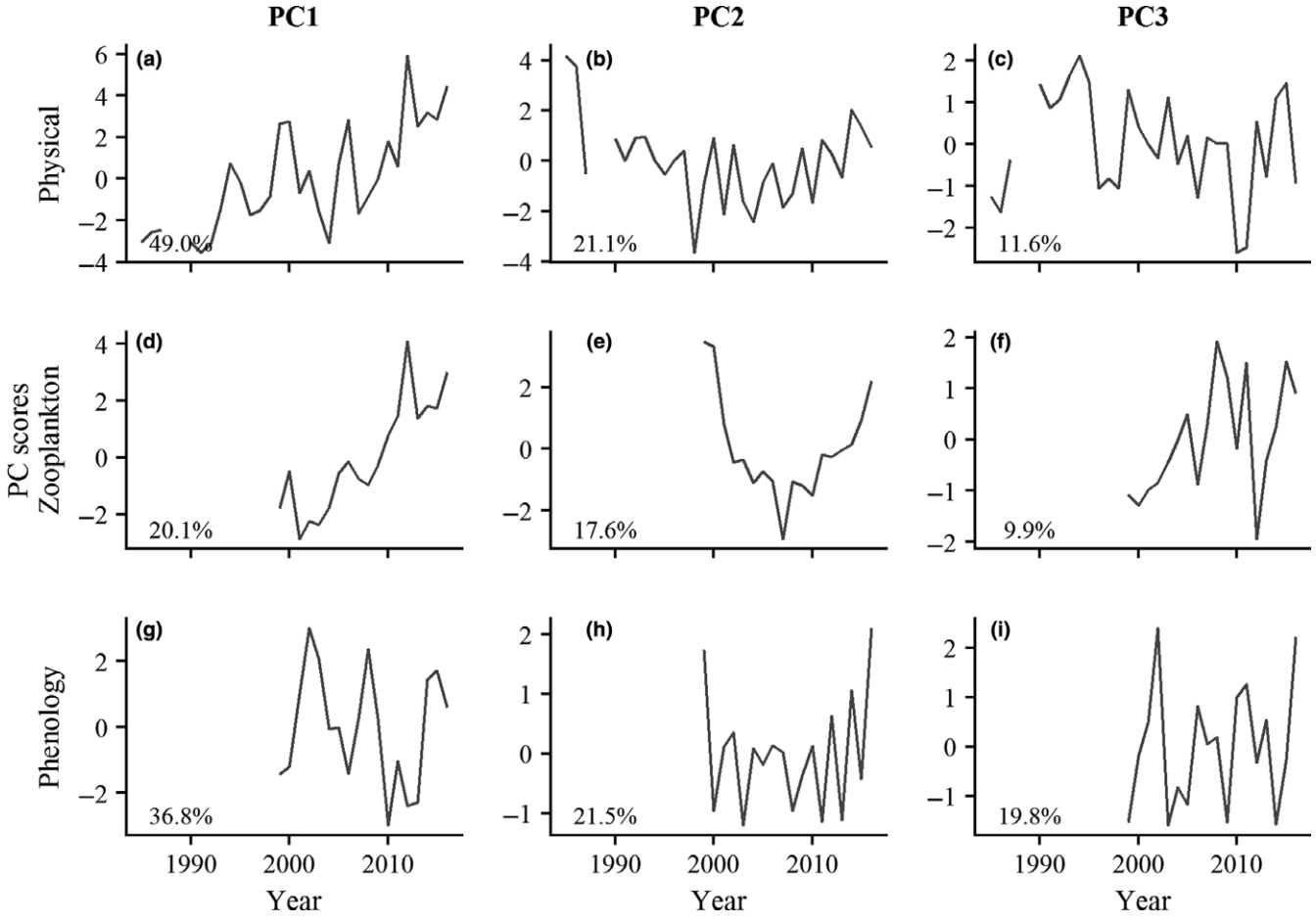

FIGURE 2 Principal component (PC) scores over time for the first three PCs for physical (a-c), zooplankton (d-f), and phenology (g-i) variable groupings. Percentages given in the bottom left denote the percentage of deviance explained by the corresponding PC

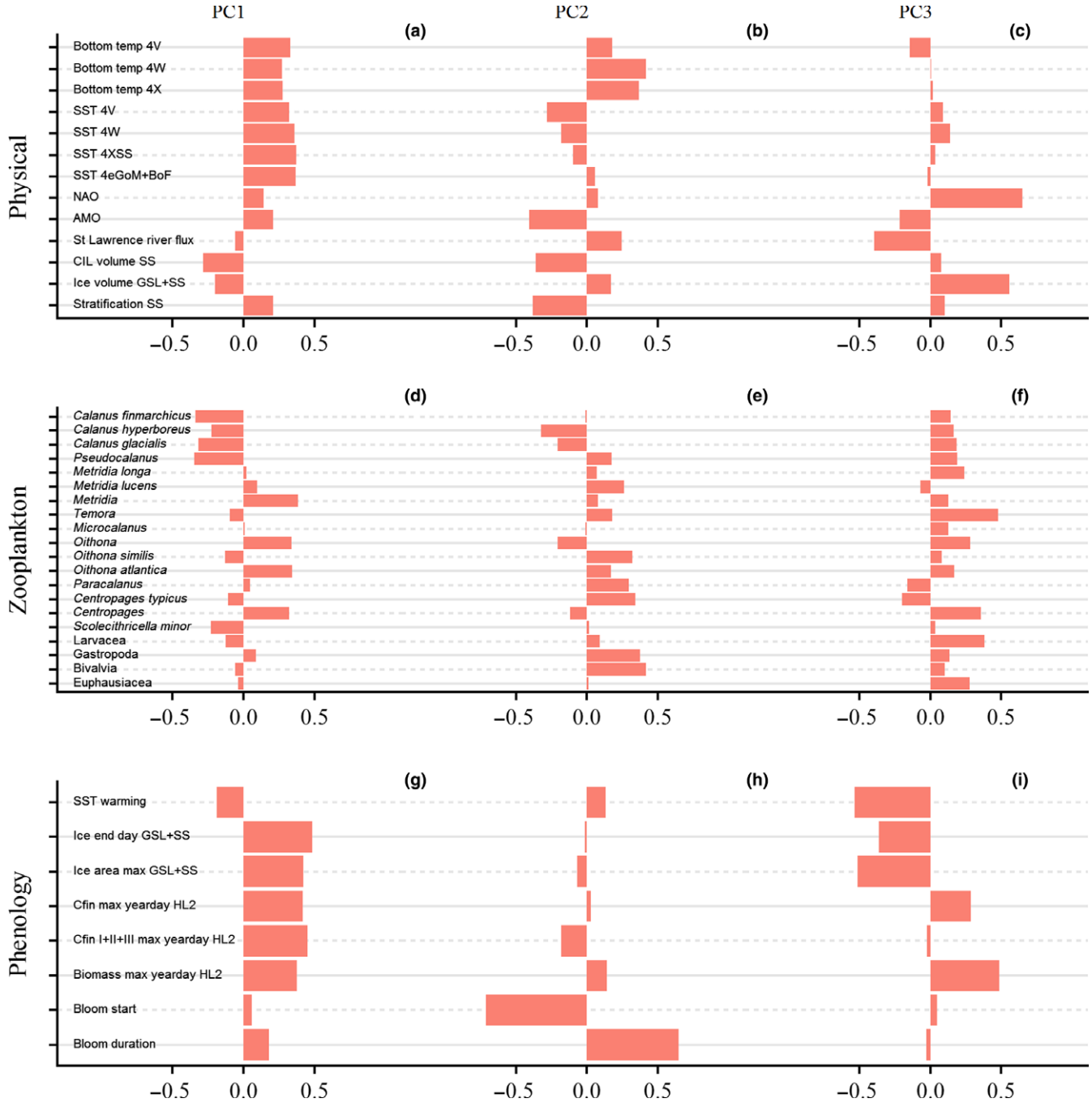

FIGURE 3 Principal component (PC) loadings for the first three PCs for physical (a-c), zooplankton (d-f), and phenology (g-i) variable groupings

As noted above, the first three PCs in zooplankton community composition explained substantially less of the variability than for the physical variables. Zooplankton PC1, which accounted for 20.1% of the variability, represented a largely positive trend over time (Figure 2d). PC1 had negative loadings for three *Calanus* species and *Pseudocalanus* sp., which are strongly associated with the spring phytoplankton bloom, and for *Temora* sp. and *Scolecithricella minor*. In addition, PC1 had positive loadings for juveniles of several taxa (*Metridia* sp., *Centropages* sp., *Oithona* sp.; Figure 3d) and *Oithona atlantica*, which are omnivores and detritivores. Noncopepod groups were not prominent in PC1. The second principal component accounted for 17.6% of the variability and was quasiparabolic in shape over the time series, with a minimum occurring around 2007 (Figure 2e). Zooplankton PC2 had negative loadings for *Calanus glacialis* and *Calanus hyperboreus* (i.e., large, arctic copepods), and positive loadings for several summer–fall copepods (*Paracalanus* sp., *Centropages typicus*), the warm-water copepod *M. lucens*, adults of both *Oithona* species, and noncopepod groups, Bivalvia and Gastropoda (Figure 3e). PC3, which accounted for 9.9% of the variability, fluctuated on a shorter time scale, exhibiting marked interannual

variability (Figure 2f). Zooplankton PC3 was most strongly associated with the small, shallow-water copepod *Temora* sp., juveniles of the small, warm-water copepod *Centropages* sp., and the noncopepod group, Larvacea. Unlike the vast majority of other taxa, which tended to have small positive loadings for this PC, *C. typicus* and *Paracalanus* sp. were negatively associated with PC3. Euphausiids, which had near-zero loadings on both PC1 and PC2, loaded positively on PC3.

The first three PCs for the phenology PCA explained nearly as much variability as the first three physical PCs, but all three were dominated by short time scale variability (Figure 2g–i). PC1 and PC3 broadly represented the timing of zooplankton and physical annual events, while PC2 represented characteristics of the spring phytoplankton bloom (Figure 3g–i). PC1 accounted for 36.8% of the variation and had positive loadings for the timing of peaks in total zooplankton biomass, *C. finmarchicus* abundance, and *C. finmarchicus* juvenile stages, as well as maximum ice area and ice end day, with high ice areas and late ice-out associated with late peaks in zooplankton biomass (Figure 3g). Phenology PC2, which accounted for 21.5% of the variation, had a positive loading on spring bloom duration and a negative loading for spring bloom initiation timing, with negative PC2 scores representing shorter, later blooms. Like PC1, PC3 was dominated by the timing of the peak in zooplankton biomass, which had a positive loading, while SST warming rate and maximum ice area and end day were negatively loaded on PC3.

3.2 | Generalized additive models

The top five GAMs for silver hake condition, adult abundance, and recruit abundance as ranked by AIC score are given in Table 2. Each response variable was described well by the model with the lowest AIC value, with a percentage of deviance explained ranging from 78.4% to 79.8%. While the optimal model for each of the silver hake metrics differs from one another, there are several common predictors as shown in a Venn diagram in Figure 4.

The top model for condition explained 78.4% of the deviance and included zooplankton PC3, phenology PC2, and physical PC3 (Table 2; Figure 5). There was a largely positive linear relationship

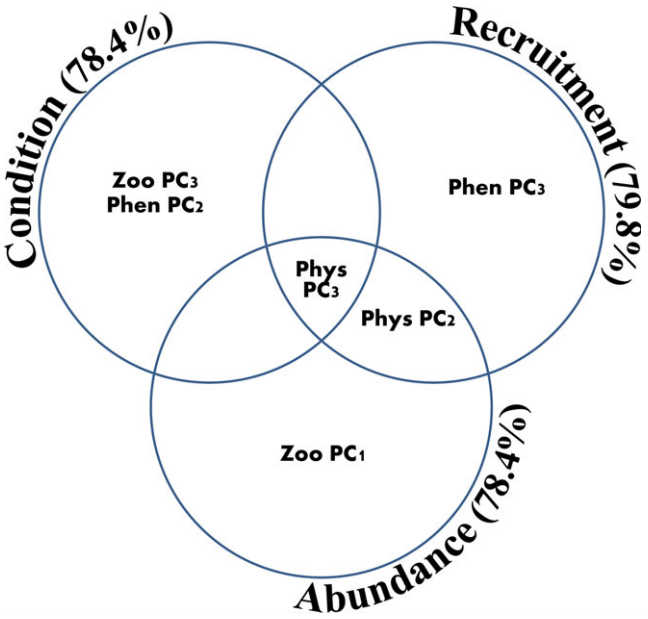

FIGURE 4 A Venn diagram showing the principal components (PCs) that are found in the optimal GAMs for silver hake condition, adult abundance, and recruitment. Percentages indicate the deviance explained by each optimal model

TABLE 2 Top five generalized additive models (GAMs) describing silver hake condition (weight at 25 cm), adult abundance, and recruitment as ranked by Akaike's information criterion (AIC). Also given are the generalized cross-validation (GCV) scores and percentage of deviance explained.

	Rank	Model			% deviance explained	AIC	GCV
Condition	1	Zooplankton PC3***	+ Phenology PC2**	+ Physical PC3#	78.4	99.8	15.4
	2	Zooplankton PC3***	+ Phenology PC2**	+ Phenology PC3#	77.6	100.1	15.5
	3	Zooplankton PC3**	+ Phenology PC2*	+ Total biomass#	77.4	101.6	17.4
	4	Zooplankton PC3**	+ Phenology PC2*		70.1	103.3	17.6
	5	Zooplankton PC3**	+ Phenology PC2*	+ Physical PC2#	73.2	104.0	19.5
Abundance	1	Physical PC2**	+ Zooplankton PC1*	+ Physical PC3*	78.4	165.4	577.9
	2	Physical PC2*	+ Zooplankton PC1**		67.8	169.4	677.2
	3	Physical PC2*	+ Zooplankton PC1#	+ Zooplankton PC3#	68.2	171.2	773.3
	4	Physical PC2*	+ Zooplankton PC1**	+ Phenology PC2#	67.9	171.3	781.0
	5	Physical PC2*	+ Zooplankton PC1**	+ Phenology PC3#	67.9	171.4	782.0
Recruitment	1	Phenology PC3**	+ Physical PC3**	+ Physical PC2**	79.8	134.7	177.9
	2	Phenology PC3*	+ Phenology PC2#	+ Adult biomass**	70.3	139.4	220.4
	3	Phenology PC3*	+ Physical PC3#	+ Adult biomass*	69.0	140.0	228.0
	4	Phenology PC3*	+ Zooplankton PC2#	+ Adult biomass*	65.3	140.7	228.4
	5	Phenology PC3*	+ Zooplankton PC1#	+ Adult biomass*	67.6	140.7	237.0

#$p > 0.05$; *$0.01 < p \leq 0.05$; **$0.001 < p \leq 0.01$; ***$p \leq 0.001$.

between condition and phenology PC2, meaning that better condition was associated with faster warming in spring and spring blooms that started earlier and lasted longer. Nevertheless, two extreme positive values of phenology PC2 caused the relationship to plateau for positive values of phenology PC2 (Figure 5b). Zooplankton PC3 had its greatest effect on the optimal model when values were large and negative and, like phenology PC2, had a positive linear relationship with condition that plateaus for positive values. Physical PC3 exhibited a positive, linear relationship with condition, but had very little impact on the optimal model over its entire range.

When the optimal model for condition was decomposed into its constituent terms, notable changes in condition (1999–2000–2001, 2013–2014) were associated with marked shifts in phenology PC2 (Figure 6). Scrutinizing PCA scores for these years (results not shown) revealed that the marked decline in condition between 1999 and 2000 was primarily due to a late bloom and, to a lesser degree, a short bloom duration. However, these factors were of comparable magnitude during the notable improvements in condition observed 2000–2001 and 2013–2014. While distinct shifts in this predictor often elicit large responses in condition, there are occasions when this is not the case, such as 2011–2012–2013. Decomposing PCA scores for these years (results not shown) revealed that shifts in phenology PC2 were driven by the timing of the bloom onset and *C. finmarchicus* production (i.e., peak in life stages CI–III), with a negligible contribution from bloom duration. Notable shifts in zooplankton PC3 tempered changes due to phenology PC2 during these years. Zooplankton PC3 describes short-term variability in the zooplankton community composition (Figure 2f) and appears in all five highest ranking models, highlighting its central role in explaining both variability of a small magnitude and large, infrequent shifts in environmental states (e.g., 2011–2012–2013). The top three models for condition all had two terms in common, zooplankton PC3 and phenology PC2, and only differed slightly in terms of AIC and deviance explained suggesting that the third terms of each model—physical PC3, phenology PC3, and total biomass—are somewhat interchangeable in this context. The fourth ranking model comprises only zooplankton PC3 and phenology PC2 and demonstrates that these terms account for the vast majority of deviance explained in the three top-ranking models.

Analysis of the residuals suggested that the optimal model was consistent with the model assumptions (Figure S3) and bootstrapping analysis demonstrated that optimal model explained significantly more deviance than random data ($p < 0.05$; Figure S4). Owing to the marked similarity among the top three models, the optimal model was often ranked second or third during the jackknife analysis (Figure S5b). This further emphasizes the important role of zooplankton PC3 and phenology PC2 in explaining variability in condition, in contrast to the largely interchangeable third covariate. In addition, there were two cases where the optimal model was ranked fourth or fifth. Nevertheless, LOOCV analysis estimated an MAE of 3.5 grams, which is ~3% of the mean weight at 25 cm between 1999 and 2016 and 60% of the standard deviation. This suggests that the

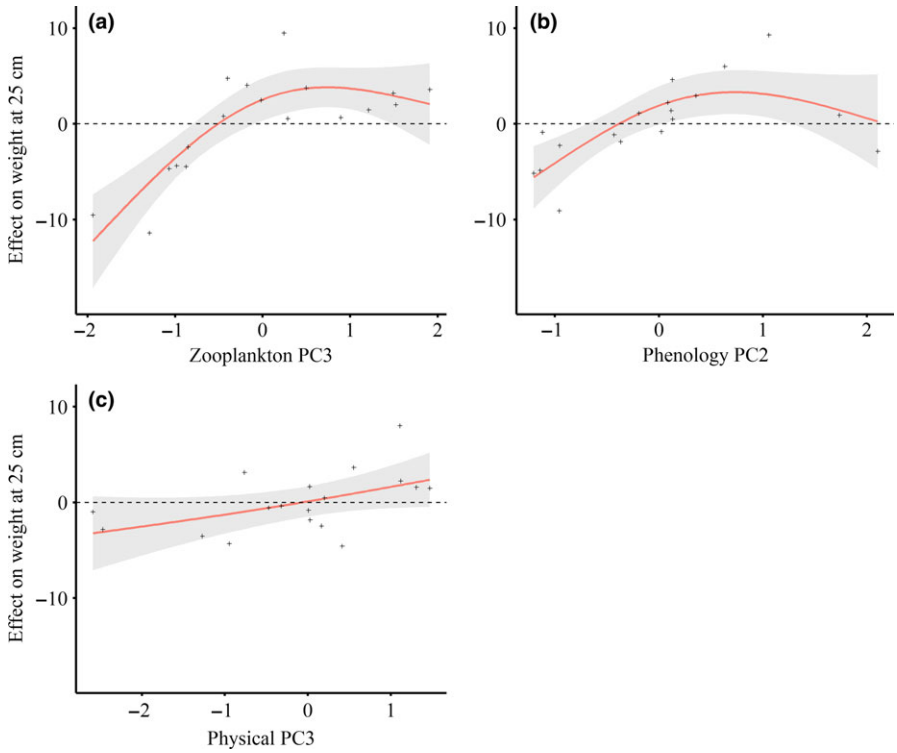

FIGURE 5 Condition (weight at 25 cm) plotted against predictors for the best performing generalized additive model (Condition ~ Zooplankton PC3 + Phenology PC2 + Physical PC3). Crosses denote observations, the solid line represents the model, and the shaded region is the 95% confidence interval. Panels a, b, and c refer to predictors zooplankton PC3, phenology PC2, and physical PC3, respectively

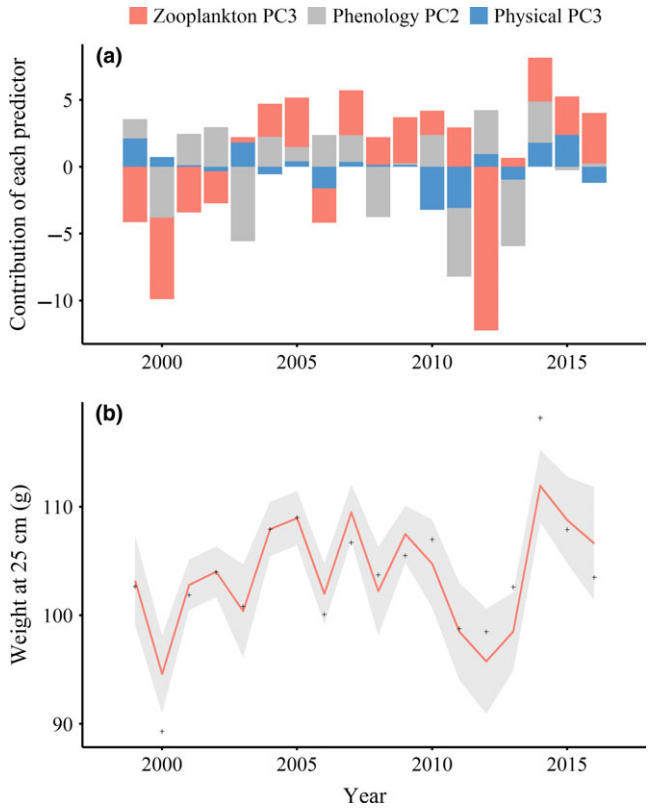

FIGURE 6 Panel a shows the contribution of each predictor in the best performing generalized additive model for condition (Condition ~ Zooplankton PC3 + Phenology PC2 + Physical PC3). Panel b shows the model (solid line; shaded area represents the 95% confidence interval) and observations (crosses) over time

model is capable of predicting condition to a relatively high degree of accuracy.

The highest ranking model for adult abundance, which explains 78.4% of the deviance, included physical PC2, zooplankton PC1, and physical PC3 (Table 2; Figure 7). Like condition, all top five GAMs for adult abundance had two terms in common—specifically, physical PC2 and zooplankton PC1. Adult abundance was shown to increase with zooplankton PC1—that is, silver hake abundance increased as biomass-dominant copepods of the *Calanus* genus declined and *Metridia*, *Centropages*, and *Oithona* copepodids and *O. atlantica* adults became more abundant. The relationship between abundance of silver hake and physical PC2 appeared somewhat U-shaped suggesting that minimal abundances were associated with intermediate values, whereas maximum abundances occurred at extreme values for the PCs. Nevertheless, these relationships were largely shaped by a single extreme observation at large positive values, and zero falls within confidence intervals at large negative values. Therefore, caution must be exercised when interpreting these results, as relationships may not persist when additional data are included. The number of silver hake adults declined as physical PC3 increased. However, confidence intervals straddle zero across almost the entire range of values suggesting a minor effect on the optimal model. Omitting this term entirely decreased the deviance explained by only 10.6%.

When decomposed into its terms (Figure 8), the optimal model for adult abundance showed that zooplankton PC1 drove a long-term increase in abundance over the time series, whereas physical PC2 was responsible for a large, episodic shift in abundance (2013–2014). Further analysis of the PC scores for these years (results not shown) revealed that this abrupt change was driven by bottom temperature for 4X/W and CIL volume (2013–2014).

The optimal model for adult abundance was consistent with the modeling assumptions (Figure S6) and explained significantly more deviance when applied to the data set than with random data (Figure S7). During the jackknife analysis, the optimal model did not rank top in three cases, when it ranked second (Figure S8). These cases tended to occur at the edge of the time series. Also, in two cases, the model was not ranked as it was omitted due to excessive concurvity. That is, a smooth term in the model could be approximated by one or more of the other smooth terms—the nonlinear analogue of multicollinearity. The MAE for the model was 32% of the mean value and 61% of the standard deviation suggesting the model performed reasonably well, but was not as accurate as the optimal model for condition.

As silver hake are recruited at 2 years of age, we first examined relationships between recruitment and environmental conditions in the two years prior to recruitment. The conditions during these years may affect spawning and/or survival at larval or early juvenile stages and, as a result, may influence the number of individuals ultimately recruited. To this end, preliminary GAMs were undertaken with lags of 0, 1, and 2 years between recruitment abundance and predictors. The optimal model with a lag of 1 year explained the greatest amount of deviance (79.8%), whereas optimal models using lags of 0 and 2 years explained only 69.6% and 66.9%, respectively, and, consequently, were not pursued further. Lagged predictors will be indicated in the results using a minus one superscript (i.e., $^{[-1]}$).

For recruitment, the top GAM, which comprised phenology PC3$^{[-1]}$, physical PC3$^{[-1]}$, and physical PC2$^{[-1]}$, explained 79.8% of the deviance (Table 2; Figure 9). All terms had very similar *p*-values. However, only phenology PC3$^{[-1]}$ appeared in all top five models. Although adult biomass$^{[-1]}$ did not feature in the optimal model, as may be expected given its previously established with recruitment (Rikhter et al., 2001), it did appear in four of the top five models, suggesting an important role in driving recruitment. All three terms in the optimal GAM had a similar form comprising linear and plateaued regions.

Figure 10 shows the optimal model for recruitment decomposed into its terms. The time series is punctuated by spikes in 2003, 2005, 2010 and 2015. Peaks in 2003, 2010, and 2015 were due to increased contributions from physical PC2$^{[-1]}$ and phenology PC3$^{[-1]}$, with physical PC3$^{[-1]}$ tempering the spike in 2015, enhancing the marked increase in 2003, and contributing little to the peak in 2010. In contrast, the 2005 peak was due to a sharp increase in physical PC3$^{[-1]}$ that was attenuated by a decrease in phenology PC3$^{[-1]}$. Higher recruitment was associated with negative values phenology PC3$^{[-1]}$ and positive values of physical PC2$^{[-1]}$ (Figure 9a, c). Together, these represented larger ice area, late ice-out, and

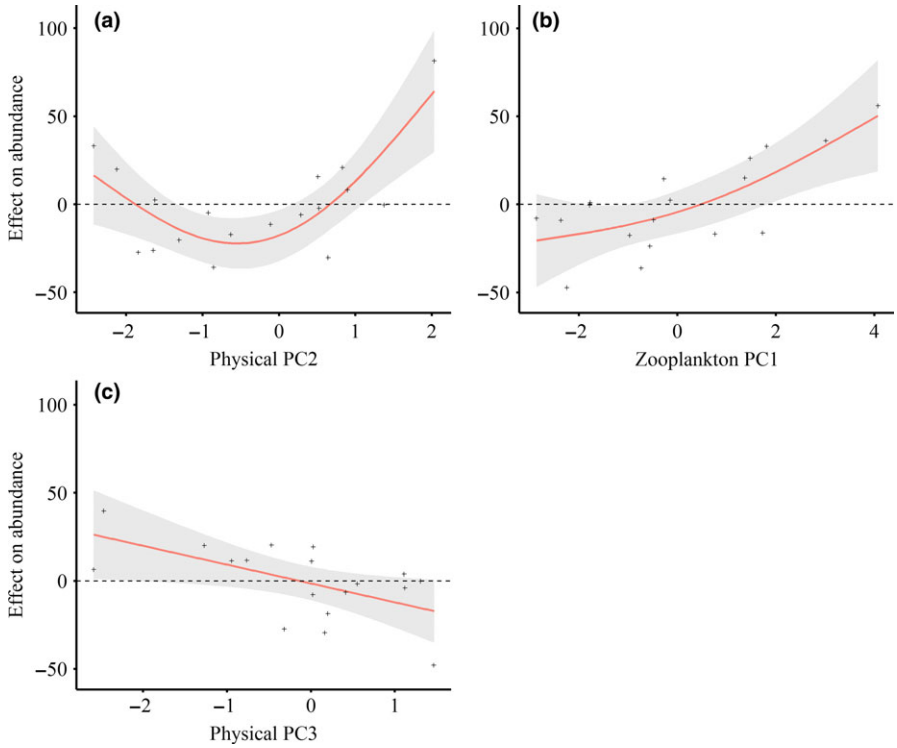

FIGURE 7 Adult abundance plotted against predictors for the best performing generalized additive model (Abundance ~ Physical PC2 + Zooplankton PC1 + Physical PC3). Crosses denote observations, the solid line represents the model, and the shaded region is the 95% confidence interval. Panels a, b, and c refer to predictors physical PC2, zooplankton PC1, and physical PC3, respectively

cooler surface waters despite faster surface warming. However, bottom waters were warmer, and stratification was reduced. In addition, the CIL volume was smaller and the AMO index was negative. Finally, the peak in zooplankton biomass occurred earlier in the year.

Analysis of residuals suggested that the optimal model for recruitment was consistent with model assumptions (Figure S9), while model validation through bootstrapping showed that the model explained more deviance than random data (Figure S10). The jackknife analysis showed that the optimal model remained ranked top in all but one case, where it ranked third, although the model was omitted on three occasions due to excessive concurvity (Figure S11). The MAE was calculated to be 8.2 million—that is, approximately one-third of the mean annual recruitment and 44% of the standard deviation. This suggests that the accuracy of the model is comparable to the optimal model for adult abundance.

For comparison to the optimal models described above, GAMs for silver hake condition, adult abundance, and recruit abundance were constructed using only physical PCs, as this afforded the use of longer time series (1985–2016 with data missing for 1988 and 1989). Despite all optimal models containing at least one physical PC and the time series increasing in length by almost 70%, these models performed much worse than the optimal models. Specifically, physical models for condition, abundance, and recruitment explained only 24.1%, 34.7%, and 15.6% of the deviance, respectively. These results emphasize the importance of including phenology and zooplankton variables in models of fish stocks.

4 | DISCUSSION

Models presented here demonstrated that environmental variability was able to explain a substantial portion of observed trends in silver hake condition, adult abundance, and recruitment. Relationships between fish metrics and predictors were often linear or domed. However, we also encountered a U-shaped relationship (i.e., Figure 7a), which is counterintuitive as it suggests that the most favorable conditions lie at opposing extremes. Nevertheless, confidence intervals at the lower end of the range straddle zero suggesting that the effect is not significant in this region and that despite appearances the relationship may not in fact be U-shaped (Figure 7a). As this relationship is largely the result of a single extreme value, caution must be exercised when interpreting these trends as they may not persist when additional data (i.e., replicates of similar extreme conditions) are included in the analysis. Nevertheless, if this relationship did persist, it may suggest that these opposing extremes may relate to favorable conditions due to different processes.

Our results demonstrated that constructing composite variables through PCA can provide a powerful means of quantifying modes of environmental variability. Environmental data should be considered representative of the variability in a range of processes that can influence fish stocks, with PCs representing the dominant modes of variability in the conditions associated with these processes even if the specific variables driving stock metrics may not be included. In some cases, such as zooplankton PC1, PCs showed a distinct

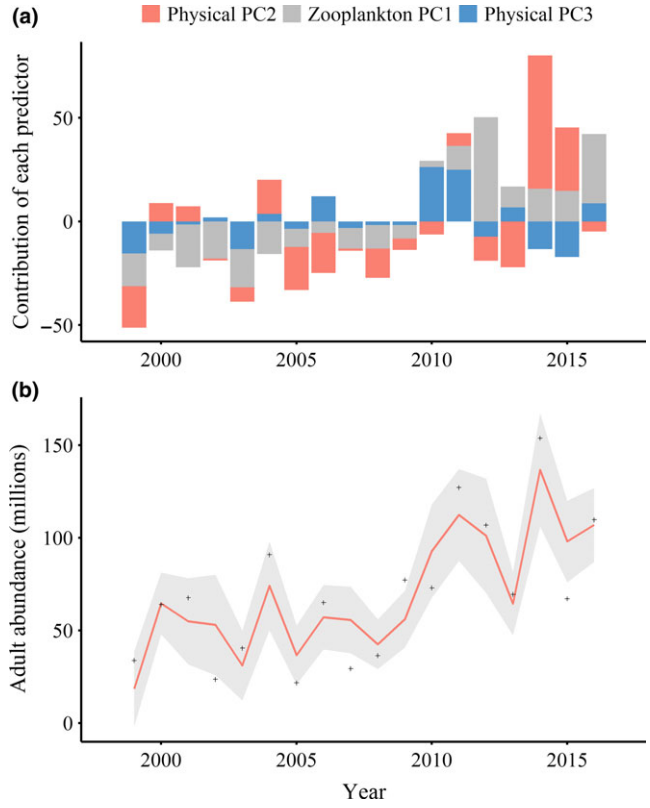

FIGURE 8 Panel a shows the contribution of each predictor in the best performing generalized additive model for abundance (Abundance ~ Physical PC2 + Zooplankton PC1 + Physical PC3). Panel b shows the model (solid line; shaded area represents the 95% confidence interval) and observations (crosses) over time

temporal trend, while others characterized multiyear or interannual variability. Validation analyses established that GAMs that used these PCs as predictors established robust relationships between fish stock metrics and environmental variability. Jackknife analyses of optimal models for abundance and recruitment identified only four instances of 35 where the optimal model did not rank as the top model. On five additional occasions, optimal models were omitted and not ranked due to excessive concurvity. Together, these tests indicate a robust modeling approach. In contrast, jackknife analysis often ranked the optimal model for condition second or third owing to the marked similarity between the top three models, which had two terms in common with their third terms being essentially interchangeable. Nevertheless, only on two occasions did the optimal model rank outside the top three demonstrating its robustness. These results highlighted the importance of considering the optimal model in the context of other high-ranking models. The fourth ranked model, which included only the two terms that appeared in all of the top-ranking models, explained less deviance than these top-ranking models (i.e., 70.1% cf. ~78%), but adopting this description of condition would explain most of the deviance while requiring fewer variables.

The three silver hake stock metric time series exhibited markedly different patterns of variability owing to the different processes modulating them. Condition chiefly reflected the timing of food availability (e.g., phenology PC2, which largely describes the onset and duration of spring phytoplankton bloom) and, consequently, exhibited short-term variability of a relatively small magnitude that was punctuated by large, episodic increases or decreases associated with infrequent yet marked changes in primary production. Similarly, recruitment showed little variation over time, but was subject to sporadic spikes that likely reflect the alignment of numerous different processes to produce favorable conditions for recruitment. However, disentangling the factors that combine to produce these notable recruitment events is very challenging (e.g., Houde, 2008; Pepin, 2016). Unlike both condition and recruitment, adult abundance exhibited a more gradual shift over time and, in addition, appeared to be independent of recruitment. For example, adult abundance reached a maximum in 2014—a substantial increase compared to 2013—yet recruitment was not notably high in the preceding year. This apparent disconnect between recruitment and abundance together with the gradual increase in abundance that is correlated with more favorable (i.e., warmer) conditions for silver hake on the Scotian Shelf suggests that observed adult abundances were influenced more by the extent of suitable habitat in the study region than by overall population size.

The GAM results highlight the importance of lower trophic level variability as a driver of silver hake stock status. Although physical PC1 characterized a strong warming trend that might be expected to influence silver hake abundance in the Scotian Shelf region related to shifts in the distribution of this warm-water stock (Nye et al., 2011), it was not included in the top model for abundance or for the other two stock metrics. Condition was influenced by phenology (PC2) and zooplankton community composition (PC3), whereas abundance was influenced mainly by zooplankton community composition (PC1) as well as shorter time scale physical variability (PC2 and PC3). Like adult abundance, recruitment was influenced by a combination of physical variability ($PC2^{[-1]}$ and $PC3^{[-1]}$), as well as phenology ($PC3^{[-1]}$) (Figure 4).

4.1 | Condition

Marked shifts in condition (e.g., 1999–2000–2001, 2013–2014) were largely driven by food availability, as suggested by the significant role of phenology PC2. This PC was chiefly associated with the onset and duration of the spring bloom (Figure 3h); high values corresponded to an early and/or long bloom, whereas low values represented a late and/or short bloom. In a broad sense, the linear portion of the relationship between phenology PC2 and condition suggested that better condition is associated with earlier and longer blooms, presumably due to an increased availability of food (Figure 5c). As surveys take place annually at the same time (i.e., July–August), an earlier bloom would allow fish to feed intensively for a longer period before sampling, resulting in better condition. Nevertheless, the relationship plateaued when phenology PC2 was large and positive, which implied that food availability was not the limiting factor in this region. While phenology PC2 provided a broad measure of productivity, euphausiids, an important component of adult silver hake's

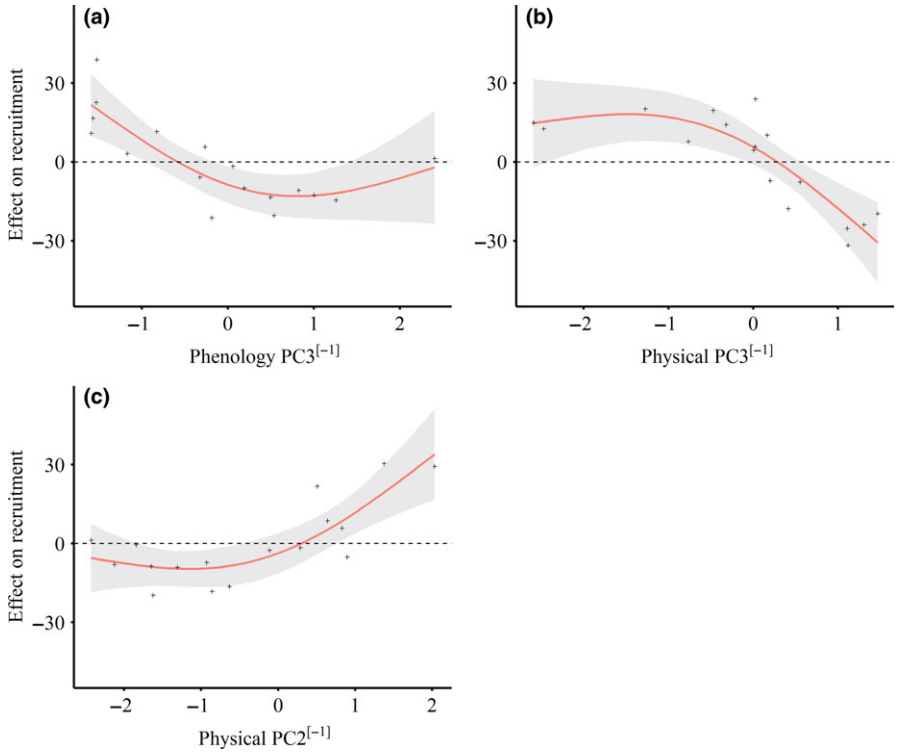

FIGURE 9 Recruitment abundance plotted against predictors for the best performing generalized additive model (Recruitment ~ Phenology $PC3^{[-1]}$ + Physical $PC3^{[-1]}$ + Physical $PC2^{[-1]}$). Crosses denote observations, the solid line represents the model, and the shaded region is the 95% confidence interval. Panels a, b, and c refer to predictors phenology $PC3^{[-1]}$, physical $PC3^{[-1]}$, and physical $PC2^{[-1]}$, respectively

diet (Vinogradov, 1993), were represented only in moderate positive loadings for zooplankton PC3 and did not emerge as a strong driver of silver hake condition. Euphausiids are highly mobile and are thus able to evade capture by the standard AZMP plankton nets (e.g., Brinton, 1967; Cochrane, Sameoto, Herman, & Neilson, 1991; Sameoto, Cochrane, & Herman, 1993; Wiebe, Boyd, Davis, & Cox, 1982). Consequently, sampling with plankton nets does not provide an accurate assessment of the euphausiid population and other sampling techniques such as acoustics-based approaches (e.g., Cochrane, Sameoto, & Herman, 2000) may prove more appropriate. Moreover, the sampling design for AZMP sections is not optimal for observing krill, which are more heterogeneously distributed than mesozooplankton, often forming very dense aggregations (McQuinn, Plourde, Pierre, & Dion, 2015; Plourde, Lehoux, Mcquinn, & Lesage, 2017).

Top-ranking models for condition were largely dictated by phenology and the composition of the zooplankton community. Total biomass appeared in only one of the top five models suggesting that density-dependent effects can play an important role for silver hake on the Scotian Shelf. This may be because density-dependent effects are often less prominent for condition than they are for other fish stock metrics, such as recruitment (Zimmermann, Ricard, Heino, & Zimmermann, 2018).

4.2 | Adult abundance

Adult abundance was driven by the long-term change in the zooplankton community (i.e., declining *Calanus* sp.) overprinted with episodic changes due to physical factors (e.g., bottom-water temperature). Adult abundance was strongly associated with zooplankton PC1, which has large negative loadings for *C. finmarchicus*, *C. hyperboreus*, *C. glacialis*, and *Pseudocalanus* sp. This relationship is consistent with previously observed negative correlations between landings of silver hake and abundances of *Calanus* sp. (Sigaev, 1994). These results are in agreement with Rikhter et al. (2001) who argued that bottom temperature was central in modulating the distribution of silver hake with food availability playing a secondary role. Indeed, both of these drivers may be characterized by zooplankton PC1 as this principal component exhibited a strong correlation (Pearson's correlation coefficient = 0.77; Figure S2) with physical PC1, which is broadly associated with warming in the region (i.e., warmer surface and bottom waters, as well as less ice and a smaller CIL volume). That is to say zooplankton PC1 may represent both declining *Calanus* sp. populations and associated warmer conditions, which may explain its selection in the five top-ranking models over physical PC1.

Sporadic shifts in abundance were often associated with changing bottom-water temperatures and large-scale climate processes. The increase in abundance between 2013 and 2014 was associated with a sharp increase in physical PC2 (Figure 9), which was chiefly due to a spike in bottom-water temperatures in NAFO region 4W—the highest value in the time series—and, to a lesser extent, a decrease in CIL volume (results not shown). Silver hake prefer warmer bottom waters and, consequently, abundances increased accordingly as previously observed by Sigaev (1994).

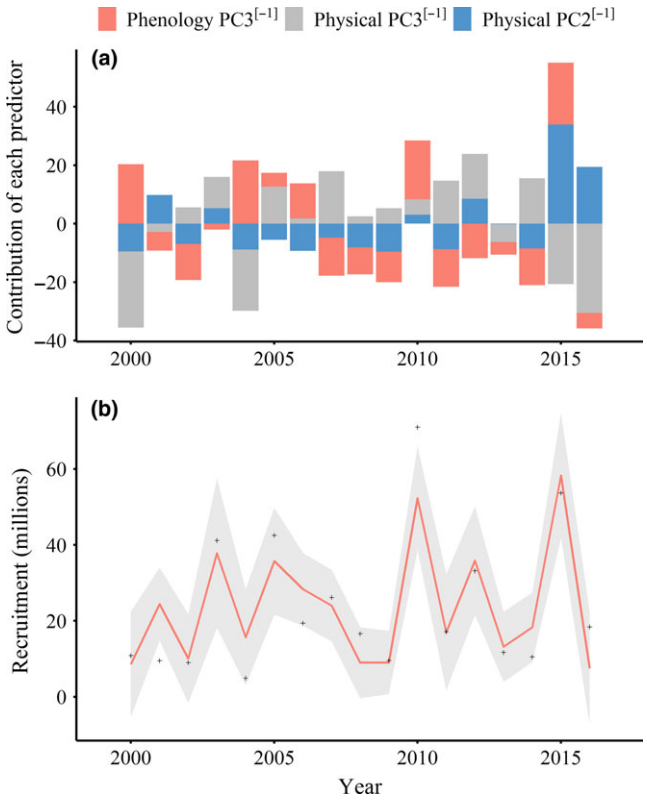

FIGURE 10 Panel a shows the contribution of each predictor in the best performing generalized additive model for recruitment (Recruitment ~ Phenology PC3$^{[-1]}$ + Physical PC3$^{[-1]}$ + Physical PC2$^{[-1]}$). Panel b shows the model (solid line; shaded area represents the 95% confidence interval) and observations (crosses) over time

4.3 | Recruitment

Recruitment was related to numerous processes: large-scale climate variability (i.e., NAO, AMO), bottom-water temperature, stratification, changes in ice indices (volume, area, and end day), SST warming, and timing of zooplankton peaks. These results are consistent with a previous study that revealed the importance of physical processes in modulating silver hake recruitment (Sigaev, 1992), but also highlight the importance of phenology. Recruitment peaks in 2003, 2010, and 2015 were largely driven by phenology PC3$^{[-1]}$ and physical PC2$^{[-1]}$. In these years, bottom-water temperature in 4W and CIL volume consistently contributed to physical PC2$^{[-1]}$, but were often accompanied by other surface-related variables with comparable magnitudes (e.g., SST 4V and 4X bottom temperature in 2003, stratification in 2010 and 2015, and ice volume in 2015), which may affect early life stages of silver hake. In contrast, phenology PC3$^{[-1]}$ shows no clear commonalities between these peak years with zooplankton biomass, SST warming, and ice end day and area being the dominant drivers in 2003, 2010, and 2015, respectively. The combination of numerous variables in driving this model underscores the complex nature of recruitment. Furthermore, recruitment is ultimately a function of both condition and abundance of the spawning population, and, consequently, the optimal model for recruitment has terms in common with the other two optimal models (Figure 4). The optimal model of recruitment that explained the greatest amount of deviance used a one year lag for predictors, suggesting that environmental conditions during the year immediately prior to recruitment (age 1–2) exerted a greater control over recruitment than environmental conditions during other years. This implies that environmental influences on juveniles are stronger drivers of silver hake recruitment than those on larval fish.

Consistent with silver hake preference for warmer conditions (Sigaev, 1994), recruitment was consistently shown to increase when bottom-water temperatures increased and the CIL declined in volume. Rikhter et al. (2001) suggested that unfavorable temperature conditions may delay spawning and decrease survival of young fish. In addition to physical processes, numerous phenology variables contributed to peaks in recruitment. Seasonal timing of food availability (i.e., peak in zooplankton biomass) was identified as an important factor (2003). Koeller, Coates-Markle, and Neilson (1989) hypothesized that physical conditions are more important during the larval stage, whereas food and growth are more important during the juvenile stage. Smaller fish fed upon copepods and, therefore, may have success with a wider variety of prey, whereas larger fish were dependent upon specific and more variable prey (i.e., amphipods, krill, and other silver hake). Abundance of juvenile silver hake has been shown to correlate with mean size of juveniles suggesting that larger size due to more favorable feeding conditions provides a survival advantage (Koeller et al., 1989). As a result, both physical factors and food availability would affect the abundance of recruits. Also, later ice end day and greater ice area were shown to be associated high recruitment (2015), which is consistent with results of similar analysis for mackerel in the Gulf of St. Lawrence (Plourde et al., 2015). However, in contrast, more rapid SST warming was also shown to be related to large recruitment events (2010). As this modeling approach cannot establish mechanistic links between environmental indices and fish stock metrics, this apparent contradiction between higher recruitment and both more rapid warming and later ice end day cannot be resolved. It may be that while both factors are important, extremely favorable conditions for one can compensate for average or unfavorable conditions in the other. Regardless, these results provide guidance in identifying potentially important relationships that can be investigated further by other means. Furthermore, it demonstrates a case when a multivariate approach is required, as each of these variables individually may not have captured the relationship.

Biomass did not feature in optimal model for recruitment presented here. However, adult biomass did appear in four of the top five ranked models suggesting density-dependent effects are important for silver hake on the Scotian Shelf. These results are in agreement with Rikhter et al. (2001) who noted that density-dependent effects on Scotian Shelf silver hake can be suppressed by physical conditions such that recruitment cannot be predicted based on spawning stock biomass, and oceanographic conditions must also be considered.

To summarize, condition is largely dictated by food availability, while adult abundance is linked to lower abundances of *Calanus* species, likely because these taxa act a proxy for key physical (e.g., bottom temperature) and plankton community attributes. Like condition, recruitment is modulated by food availability but is also a function of adult biomass and physical attributes. Adult abundance has increased gradually with time and does not exhibit the sporadic peaks observed in the recruitment, suggesting that adult abundance reflects the availability of suitable pelagic habitat rather than the population size. That is, our metric of abundance may be strongly influenced by changes in distribution in addition to changes in the overall number of adults in the stock.

4.4 | Overarching perspective

The predictive ability of the approach adopted here relies on identifying dominant patterns in the PCs that drive optimal models. While these PCs may only explain a relatively small amount of variance in the data set, bootstrapping analysis suggests that GAMs built from these PCs are robust and that the variance that is important for explaining fish stock metrics is adequately characterized by the PCAs. Similarly, the time series considered here are relatively short, but are generally robust as shown by the jackknife analysis. The jackknife analysis is particularly useful for the recruitment and condition time series, as it quantifies the impact of extreme values of model selection and performance. Although longer time series would include more episodic, extreme observations and, consequently, lead to a more robust optimal model, the models derived with the current time series were shown to be resilient to extreme values.

Silver hake abundance was strongly associated with zooplankton PC1, which represents, in part, a long-term decline in the abundance of *Calanus* species since 1999. As *Calanus* species are not an important component of the silver hake diet, this long-term trend may instead reflect other changes in other key environment variables. For example, the decline of *Calanus* species may be associated with the warming of Scotian Shelf waters, but it may also indicate a fundamental change in flow of energy through the food web, potentially to the benefit of taxa such as krill that are not well sampled. This trend was associated with gradual improvement in silver hake abundance over time, although it was overprinted by sporadic changes in physical indices, which exert a marked influence. If the zooplankton trend continues into the future—and waters are expected to continue warming—we would anticipate that silver hake abundance would continue to increase in this region. However, in contrast to abundance, condition has been relatively constant over time with sporadic shifts associated with food availability and short-term variability in zooplankton community composition. Identifying trends in PCs that exhibit marked interannual variability such as these is substantially more difficult. Similarly, recruitment was largely driven by shifts in phenology and physical metrics that do not exhibit clear long-term trends. Complicating predictions of both recruitment and condition is the observation that peaks are typically associated with the alignment of several terms that in others years counter one another, whereas abundance exhibits a more straightforward relationship with the environment.

5 | FISHERIES ADVICE

Scoping the environmental and ecosystem attributes that influence stock productivity, distribution, and abundance is a critical first step toward implementing an ecosystem approach to stock assessment and the provision of fisheries advice. The formal incorporation of ecosystem characteristics into stock assessment advice has been accomplished both qualitatively (e.g., Choi, Frank, Petrie, & Leggett, 2005) and quantitatively (e.g., Miller, Hare, & Alade, 2016). Qualitative addition of ecosystem characteristics will typically frame the discussion around the relative risk of different harvest strategies, without placing the results in a probabilistic setting. There is value in having qualitative ecosystem considerations in stock assessments as the various stakeholders are informed of the external factors which may, in the short, medium, or long term, impact stock productivity. In quantitative assessments, the incorporation of a time series of ecosystem characteristics typically occurs as a covariate used to describe the annual deviations to parameters such as natural mortality (Deriso, Maunder, & Pearson, 2008) to partition parameters' variance and obtain improved maximum likelihood estimates. The preceding analysis provides information on the functional form and directionality of key ecosystem considerations for silver hake, all of which are key to implementing quantitative stock assessments. In its present form, the Scotian Shelf silver hake stock assessment is conducted as a biomass dynamic model, which combines total commercial biomass indices from the fisheries independent scientific surveys as well as the total landings from the fishery. As currently implemented, these environmental covariates cannot readily be integrated into model structure. However, the results presented here form the basis for qualitative assessment of ecosystem attributes and the influence on silver hake stock productivity. Future work will seek to incorporate the relationships between condition, adult abundance, and recruitment with environmental and ecosystem conditions into a quantitative assessment model.

ACKNOWLEDGEMENTS

This work was supported by DFO's Aquatic Climate Change Adaptation Services Program (ACCASP). Ocean observations were made by DFO's Atlantic Zone Monitoring Program (AZMP) and silver hake population metrics were collected during DFO Research Vessel Surveys with support from the captains and crew of Canadian Coast Guard and from DFO data management groups. Oceanographic metrics were provided by Peter Galbraith, Dave Hebert, Roger Pettipas, Eugene Colbourne, and the Bedford Institute of Oceanography operational remote sensing group. We thank two anonymous reviewers for their constructive comments, which improved this manuscript. The authors declare no conflict of interests.

ORCID

Catherine Johnson http://orcid.org/0000-0001-5291-3141

REFERENCES

Brinton, E. (1967). Vertical migration and avoidance capability of euphausiids in the California Current. *Limnology and Oceanography*, *12*, 451–483. https://doi.org/10.4319/lo.1967.12.3.0451

Brosset, P., Doniol-Valcroze, T., Swain, D. P., Lehoux, C., Van Beveren, E., Mbaye, B. C., … Plourde, S. (2018). Environmental variability controls recruitment but with different drivers among spawning components in Gulf of St. Lawrence herring stocks. *Fisheries Ocenanography*. Advance online publication. https://doi.org/10.1111/fog.12272

Brown, C. J., Fulton, E. A., Possingham, H. P., & Richardson, A. J. (2012). How long can fisheries management delay action in response to ecosystem and climate change ? *Ecological Applications*, *22*(1), 298–310. https://doi.org/10.1890/11-0419.1

Choi, J. S., Frank, K. T., Petrie, B. D., & Leggett, W. C. (2005). Integrated assessment of a large marine ecosystem: A case study of the devolution of the Eastern Scotian Shelf, Canada. *Oceanography and Marine Biology: An Annual Review*, *43*, 47–67.

Clay, D., Currie, L., & Swan, B. (1984). Food and feeding of Silver hake (*Merluccius bilinearis* Mitchill), on the Scotian Shelfmith special reference to Cannibalism. Northwest Atl. Fish. Organ. Sci. Counc. Stud. Serial No. (86): 25.

Cochrane, N. A., Sameoto, D. D., & Herman, A. W. (2000). Scotian Shelf euphausiid and silver hake population changes during 1984-1996 measured by multi-frequency acoustics. *ICES Journal of Marine Science*, *57*(1), 122–132. https://doi.org/10.1006/jmsc.1999.0563

Cochrane, N., Sameoto, D., Herman, A., & Neilson, J. (1991). Multiple-frequency acoustic backscattering and zooplankton aggregations in the inner Scotian Shelf Basins. *Canadian Journal of Fisheries and Aquatic Science*, *48*, 340–355. https://doi.org/10.1139/f91-046

Deriso, R. B., Maunder, M. N., & Pearson, W. H. (2008). Incorporating covariates into fisheries stock assessment models with application to pacific herring. *Ecological Applications*, *18*(5), 1270–1286. https://doi.org/10.1890/07-0708.1

DFO. (2017). Scotian Shelf Silver Hake (NAFO Divisions 4VWX) Stock Status Update for 2016–2017. DFO Can. Sci. Advis. Sec. Sci. Resp. 2017/010.

Gatien, M. G. (1976). A study in the slope water region south of Halifax. *Journal of the Fisheries Research Board of Canada*, *33*, 2213–2217. https://doi.org/10.1139/f76-270

Hare, S. R., & Mantua, N. J. (2009). Empirical evidence for North Pacific regime shifts in 1977 and 1989. *Progress in Oceanography*, *47*(2000), 103–145.

Hebert, D., Pettipas, R., Brickman, D., & Dever, M. (2016). Sea ice and physical oceanographic conditions on the Scotian Shelf and in the Gulf of Maine during 2015. DFO Can. Sci. Advis. Sec. Res. Doc. (2015/040): v + 49.

Houde, E. D. (2008). Emerging from Hjort's Shadow. *Journal of Northwest Atlantic Fishery Science*, *41*, 53–70. https://doi.org/10.2960/J.v41.m634

Hurrell, J. W. (1995). Decadal trends in the North Atlantic Oscillation: Regional temperatures and precipitation. *Science*, *269*, 679.

Johnson, C., Devred, E., Casault, B., Head, E., & Spry, J. (2018). Optical, chemical, and biological oceanographic conditions on the Scotian Shelf and in the Eastern Gulf of Maine in 2016. DFO Can. Sci. Advis. Sec. Res. Doc. 2018/017: vi + 58 p.

Koeller, P., Coates-Markle, L., & Neilson, J. (1989). Feeding ecology of juvenile (age-0) Silver Hake (*Merluccius bilinearis*) on the Scotian Shelf. *Canadian Journal of Fisheries and Aquatic Science*, *46*, 1762–1768. https://doi.org/10.1139/f89-223

McLellan, H. (1957). On the distinctness and origin of the slope water off the Scotian Shelf and its Easterly Flow South of the Grand Banks. *Journal of the Fisheries Research Board of Canada*, *14*, 213–239. https://doi.org/10.1139/f57-011

McLellan, H., Lauzier, L., & Bailey, W. (1953). The slope water off the Scotian Shelf. *Journal of the Fisheries Research Board of Canada*, *11*, 155–176. https://doi.org/10.1139/f53-012

McQuinn, I. H., Plourde, S., Pierre, J. S., & Dion, M. (2015). Progress in Oceanography Spatial and temporal variations in the abundance, distribution, and aggregation of krill (*Thysanoessa raschii* and *Meganyctiphanes norvegica*) in the lower estuary and Gulf of St. Lawrence. *Progress in Oceanography*, *131*, 159–176. https://doi.org/10.1016/j.pocean.2014.12.014

Miller, T. J., Hare, J. A., & Alade, L. A. (2016). A state-space approach to incorporating environmental effects on recruitment in an age-structured assessment model with an application to southern New England yellowtail flounder. *Canadian Journal of Fisheries and Aquatic Science*, *73*, 1261–1270. https://doi.org/10.1139/cjfas-2015-0339

Mitchell, M. R., Harrison, G., Paule, K., Gagné, A., Maillet, G., & Strain, P. (2002). Atlantic zonal monitoring program sampling protocol. Canadian Technical Report of Hydrography and Ocean Sciences 223: iv + 23. Available from ISSN 071 1-6764.

Myers, R. A. (1998). When do environment-recruitment correlations work? *Review in Fish Biology and Fisheries*, *8*, 285–305. https://doi.org/10.1023/A:1008828730759

Nye, J. A., Joyce, T. M., Kwon, Y.-O., & Link, J. S. (2011). Silver hake tracks changes in Northwest Atlantic circulation. *Nature Communications*, *2*, 412. https://doi.org/10.1038/ncomms1420

Pepin, P. (2016). Reconsidering the impossible—Linking environmental drivers to growth, mortality, and recruitment of fish. *Canadian Journal of Fisheries and Aquatic Science*, *73*, 205–215. https://doi.org/10.1139/cjfas-2015-0091

Petrie, B., Smith, P. C., Petrie, B., & Smith, P. C. (1977). Low-frequency motions on the Scotian shelf and slope. *Atmosphere (Basel)*, *15*(3), 117–140.

Plourde, S., Grégoire, F., Lehoux, C., Galbraith, P. S., Castonguay, M., & Ringuette, M. (2015). Effect of environmental variability on body condition and recruitment success of Atlantic Mackerel (*Scomber scombrus* L.) in the Gulf of St. Lawrence. *Fisheries Ocenanography*, *24*(4), 347–363. https://doi.org/10.1111/fog.12113

Plourde, S., Lehoux, C., Mcquinn, I. H., & Lesage, V. (2017). Describing krill distribution in the western North Atlantic using statistical habitat models. DFO Can. Sci. Advis. Sec. Res. Doc. 2016/111(January): v + 34 p.

R Development Core Team. (2016). *R: A language and environment for statistical computing*. Vienna, Austria: R Foundation for Statistical Computing.

Rikhter, V. A., Sigaev, I. K., & Vinogradov, V. A. (2001). Silver hake of Scotian Shelf: Fishery, environmental conditions, distribution, and biology and abundance dynamics. *Journal of Northwest Atlantic Fishery Science*, *29*, 51–92. https://doi.org/10.2960/J.v29.a5

Rose, K. A. (2000). Why are quantitative relationships between environmental quality and fish populations so elusive? *Ecological Applications*, *10*(2), 367–385. https://doi.org/10.1890/1051-0761(2000)010[0367:WAQRBE]2.0.CO;2

Sameoto, D., Cochrane, N., & Herman, A. (1993). Convergence of acoustic, optical, and net-catch estimates of euphausiid abundance: Use of artificial light to reduce net avoidance. *Canadian Journal of Fisheries and Aquatic Science*, *50*(2), 334–346. https://doi.org/10.1139/f93-039

Schlesinger, M. E., & Ramankutty, N. (1994). An oscillation in the global climate system of period 65-70 years. *Nature*, *367*, 723–726. https://doi.org/10.1038/367723a0

Sigaev, I. K. (1992). On possible causes of year-class variability of Scotian Shelf silver hake (*Merluccius bilinearis*). *Journal of Northwest Atlantic Fishery Science*, *13*, 103–105. https://doi.org/10.2960/J.v14.a7

Sigaev, I.K. (1994). Distribution of Silver Hake, water temperatures, and Zooplankton on the Scotian Shelf in May-June 1993. NAFO Scientific Council Studies No. 23: 1–7.

Skern-Mauritzen, M., Ottersen, G., Handegard, N. O., Huse, G., Dingsør, G. E., & Nils, C. (2016). Ecosystem processes are rarely included in tactical fisheries management. *Fish and Fisheries*, *17*, 165–175. https://doi.org/10.1111/faf.12111

Smith, P. C., Petrie, B., & Mann, C. R. (1978). Circulation, variability, and dynamics of the Scotian Shelf and slope. *Journal of the Fisheries Research Board of Canada*, *35*, 1067–1083. https://doi.org/10.1139/f78-170

Stone, H. H., Themelis, D., Cook, A. M., & Clark, D. S. (2013). Silver hake 2012 framework assessment: Data inputs and exploratory modelling. DFO Can. Sci. Advis. Sec. Res. Doc. 2013/008(November): v + 133.

Sutton, R. T., & Hodson, D. L. R. (2013). Atlantic Ocean forcing of North American and European summer climate. *Science*, *309*, 115–118. https://doi.org/10.1126/science.1109496

Therriault, J., B., P., Pepin, P., Gagnon, J., Gregory, D., Helbig, J., … Sameoto, D. (1998). Proposal for a northwest Atlantic zonal monitoring program. Can. Tech. Rep. Hydrogr. Ocean Sci. 194: vii+57p.

Vinogradov, V. I. (1993). On hake feeding related to distribution of food organisms in the Scotian Shelf area in 1988, 1990. NAFO SCR Doc., No. 7, Serial No. N2182.

Wiebe, P. H., Boyd, S. H., Davis, B. M., & Cox, J. L. (1982). Avoidance of towed nets by the euphausiid Nematoscelis megalops. *Fishery Bulletin*, *80*(1), 75–91.

Wood, S. N. (2006). *Generalized additive models: An introduction with R*. London, UK: Chapman and Hall.

Zhai, L., Platt, T., Tang, C., Sathyendranath, S., & Herna, R. (2017). Phytoplankton phenology on the Scotian Shelf. *ICES Journal of Marine Science*, *68*, 781–791.

Zimmermann, F., Ricard, D., Heino, M., & Zimmermann, F. (2018). Density regulation in Northeast Atlantic fish populations: Density dependence is stronger in recruitment than in somatic growth. *Journal of Animal Ecology*, *87*, 672–681. https://doi.org/10.1111/1365-2656.12800

SUPPORTING INFORMATION

Additional supporting information may be found online in the Supporting Information section at the end of the article.

How to cite this article: Reed D, Plourde S, Cook A, et al. Response of Scotian Shelf silver hake (*Merluccius bilinearis*) to environmental variability. *Fish Oceanogr*. 2018;00:1–17. https://doi.org/10.1111/fog.12406